DISTRIBUTED MODEL PREDICTIVE CONTROL FOR ENERGY SYSTEMS IN MICROGRIDS

PAUL STADLER, ARAZ ASHOURI, AND FRANCOIS MARÉCHAL

ABSTRACT. This paper presents a flexible and modular control scheme based on distributed model predictive control (DMPC) to achieve optimal operation of decentralized energy systems in smart grids. The proposed approach is used to coordinate multiple distributed energy resources (DERs) in a low voltage (LV) microgrid and therefore, allow virtual power plant (VPP) operation. A sequential and iterative DMPC formulation is shown which incorporates global grid targets along with the local comfort requirements and performance indices. The preliminary results generated by the simulation of a studied case proves the benefits of applying such a control scheme to a benchmark low voltage microgrid.

1. Introduction

The progressive shift towards decentralized generation in power distribution networks has rendered the problem of optimal operation of distributed energy resources (DERs) to be increasingly constraining. Indeed, the integration of flexible deterministic energy systems combined with the strong penetration of uncontrollable and stochastic renewable energy sources (RESs) has pushed the gird to its operating limits [1]. Micro grids represent a promising concept to face the latter issue; by interconnecting and thus monitoring the different DERs, the aggregated operation strategy enables the provision of voltage support and other ancillary services to the local distribution system operator (DSO) [2, 3, 4, 5]. Nevertheless, the growing integration of polygeneration systems (e.g. combined heat and power units) and heat pumps raises the need of considering both electrical and thermal power requirements while establishing optimal operation strategies.

Several studies have proposed robust control mechanisms to achieve stable operation of low-voltage (LV) microgrids to cope with the abovementioned objectives. From the DSO perspective, centralized hierarchical control schemes are commonly selected (e.g. [4, 6]), establishing set points for the DER load profiles to reach the grid operational targets. The results presented in [7] demonstrated the advantage of implementing the following control strategy; the voltage profiles at the grid buses are highly improved through optimal DERs scheduling. However, regarding the interest of DER owners connected to the microgrid, local strategies may highly differ from the DSO operating objective [6]. From the point—of—view of the end-user (e.g. a residential building), model predictive control (MPC) architectures are usually applied to minimize operating costs while satisfying the different comfort and service requirements of the smart grid actor (e.g. [8, 9, 10, 11]). Nevertheless, a lack of communication between the different MPC units while defining the local strategies might cause critical grid operating conditions [3]. In order to face these issues, authors in [12] presented a distributed model predictive control (DMPC) architecture,

Date: August 21, 2018.

The authors are with the Swiss Federal Institute of Technology Lausanne (EPFL), Sion, Switzerland. Emails: paul.stadler@epfl.ch, ashouri@alumni.ethz.ch, francois.marechal@epfl.ch.

coordinated through an independent system operator (ISO) in order to steer towards a global grid objective of peak-shaving. However, a robust control regarding the violation of power flow limit in the LV network slack bus and variable bound setting are not discussed in that study.

This paper presents a flexible, modular and robust control architecture based on an DMPC problem formulation [13]. The fully connected, iterative and independent MPC algorithm establishes the optimal set points of the controllable DERs connected to the LV microgrid. Besides optimizing the local control objectives, the coordination of the regulators allows the ISO to act as a virtual power plant (VPP) while providing ancillary services to the DSO. Indeed, by supplying day-ahead load predictions – computed considering a cost performance index – to the DSO, it is able to act with more certainty in the electricity market. The structure of the paper is the following: Section II explains the control scheme and Section III defines the case study considered. Section IV shows the advantages of using the proposed DMPC through simulation results. Section V finally provides concluding comments about of the proposed control method.

2. Control Algorithm

In addition to avoiding a conflict of interests among the different DER owners and the local DSO [6], the major advantage of the decentralized control remains in the computational effort required to solve the problem formulation [12, 13]. In fact, by splitting the large, centralized optimization process into multiple, smaller sub-problems, solving time and flexibility of the MPC is strongly improved. Nevertheless, in order to ensure that local actions are not threatening the global system stability, coordination between the different regulators is still required to satisfy specific coupling constraints. As presented in [15], several control schemes have been proposed to cope with the coordination challenges. Nevertheless, no generic design approach has yet been developed, leading to only case-specific, tailored DMPC problem formulations.

The DMPC architecture proposed in this paper relies on the combination of a sequential and iterative solving approach. As discussed in [15], regarding the information exchanged, the local regulators require comprehensive models of the different subsystems. Nevertheless, given the global system objective considered in this study, solely the future predicted control variables need to be transmitted to the different controllers, without any knowledge of the other

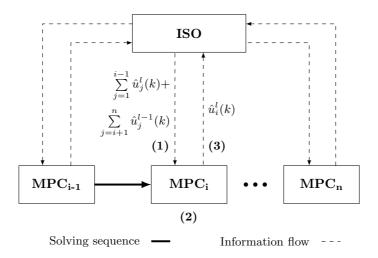


FIGURE 1. DMPC computation scheme.

DER models. Since the defined coupling constraint solely relates to the net power flow at each bus, efforts concerning the exchange of information and controller synchronization are strongly improved. The following paragraph details the specific DMPC algorithm developed for the optimal operation of DER units located in an LV microgrid.

2.1. **DMPC** architecture. In the presented control algorithm, the local regulators are monitored through an ISO which stores the predicted load profiles of the MPCs connected to the microgrid. The latter independent grid agent solely consists of a simple data managing system, representing the aggregated interests of the local network actors. To solve the DMPC problem, a sequential updating approach [12] is applied during which each regulator solely interacts with the ISO. As shown in Figure 1, the MPC hence calls the central ISO to gather the previously predicted operating plans of the remaining DERs (1), computes the local strategy (2) before submitting it to the ISO (3).

This process is performed in an iterative manner until the aggregated load plan variance perceived by the ISO reaches the defined convergence criteria ϵ (Algorithm 1). In order to initialize the solving scheme for the first iteration (i.e. l=1), the operation plan defined during the previous time step, $\sum \hat{u}^l(k-1)$, is considered for units located later in the solving scheme. Each controller solves a standard MPC problem formulation. Also as shown in [16], the performance index is composed of local objectives and an aggregated input target (1). The thermal and electrical loads related to the local DER and service requirements are computed considering a 1 hour time step (sampling time) with a 24 hours prediction horizon. The control inputs u_i are defined as simply being the actual state of operation/charge of the different DERs within the subsystem (i.e. building) i. In order to prioritize thermal comfort requirements, a strong penalty cost is applied when violating the soft constraint (3).

3. Case Study

This case study presents the optimal operation of multiple DERs connected to an LV microgrid through flexible DMPC. The global objective of the distributed control architecture is to provide the day-ahead, aggregated load profile to the respective DSO of the LV network through the grid ISO. The forecasted consumption curve highly improves the DSO bargaining power on the daily electricity market since the future load profile is assumed to be determined *a priori*. In exchange for the transmitted information, the microgrid end-users might benefit from a reduced electricity tariff or similar economic incentives from the local DSO.

To reach the microgrid forecasted load profile, the DMPC regulators are however constrained to respect the aggregated consumption predictions and thus, need to steer towards the defined profile. In order to account for the stochastic related to the specific end-user behavior, the aggregated consumption is allowed to vary within a predefined band in which no penalty is perceived by the microgrid. Nevertheless, when exceeding the upper or lower profile limit, a non-compliance fee (Table 2) is charged to the ISO since the economic advantage of the DSO has vanished. Hence, in the following case study, each grid bus (i.e. end-user) is equipped with an MPC regulator which optimizes the hybrid performance index (Eq. 1) which includes the local operating expenses (Eq. 2) and comfort penalties (Eq. 3) in addition to the global non-compliance cost (Eq. 4):

(1)
$$\begin{cases} J\left(X_{i}(k), U_{i}(k), \sigma_{i}(k)\right) = f_{opex}\left(U_{i}(k)\right) + f_{conf}\left(X_{i}(k)\right) + f_{grid}\left(U_{i}(k), \sigma_{i}(k)\right) \\ X_{i}(k) = \left\{\hat{x}_{i}(k+1|k), ..., \hat{x}_{i}(k+N|k)\right\} \\ U_{i}(k) = \left\{\hat{u}_{i}(k|k), ..., \hat{u}_{i}(k+N-1|k)\right\} \end{cases}$$

(2)
$$f_{opex}(U_i(k)) = c_{el}(k)(\hat{P}_i^+(k) - \hat{P}_i^-(k)) + c_{fuel}(k)\hat{m}_{fuel}^+(k)$$

(3)
$$f_{conf}(X_i(k)) = c_{p,conf}|\bar{T}_i(k) - \hat{T}_i(k)|$$

(4)
$$f_{grid}(U_i(k)) = c_{p,grid} \left| \bar{P}_i^+(k) - \left(\hat{P}_i^+(k) + \sum_{j=1, i \neq j}^n \hat{P}_j^+(k-1) \right) \right|$$

where the symbol $\hat{}$ indicates the predicted values of the corresponding state, x, and input, u, while +/- superscripts indicate specific input and output flows (e.g. power, P) respectively.

Algorithm 1: DMPC algorithm

```
Data:
```

end

```
- R Controller set, R \in \mathbb{N}^*
```

- l Main loop iterator
- $U^{l}(k)$ Aggregated load profile of all controllers at time step k
- $\sigma_i^l(k)$ Aggregated load profile of controllers $j, j \in R \{i\}$
- $\hat{u}_i^l(k)$ Predicted load profile of controller i at time step $k, i \in R$

```
Result: \hat{u}_i(k), i \in R

Initialize: l = 0, U^0(k) = 0;

while U^l(k) - U^{l-1}(k) < \epsilon do
 \begin{vmatrix} l = l + 1; \\ \text{for } i = 1 \text{ to } n \text{ do} \\ & \begin{vmatrix} \sigma_i^1(k) = \sum\limits_{j=1}^{i-1} \hat{u}_j^1(k) + \sum\limits_{j=i+1}^n \hat{u}_j^1(k-1); \\ \text{else} \\ & \begin{vmatrix} \sigma_i^l(k) = \sum\limits_{j=1}^{i-1} \hat{u}_j^l(k) + \sum\limits_{j=i+1}^n \hat{u}_j^{l-1}(k); \\ \text{end} \\ & \text{Compute MPC}_i(X_i^l(k), U_i^l(k), \sigma_i^l(k)); \\ & \text{Submit } \hat{u}_i^l(k) \text{ to ISO}; \\ & \text{end} \\ & U^l(k) = \sum\limits_{i=1}^n \hat{u}_i^l(k) \\ \end{vmatrix}
```

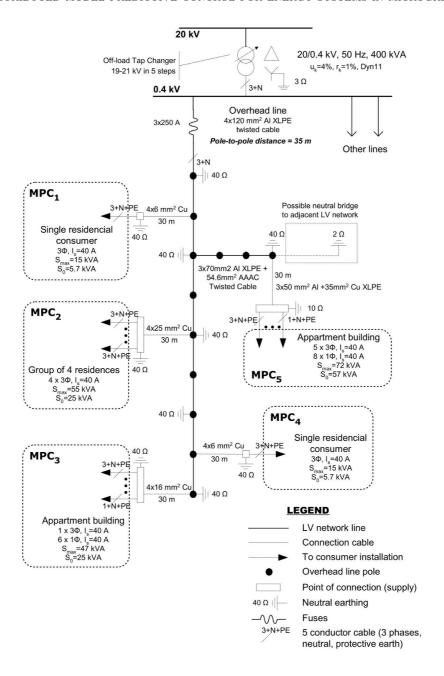


FIGURE 2. Low-Voltage microgrid network structure [15].

3.1. **System description.** The system considered in this case study is composed of 8 buildings 6 single family houses (SFHs) and 2 multi-family houses (MFHs) connected to a small network. The different DER types located at each grid bus/buildings are presented in Table 1. The simulations are performed on an IEEE benchmark LV network (Figure 2) proposed by the CIGRE research group [15]. The different building and DER models proposed in [3, 9, 17, 18] have been implemented in the following simulations.

SFH

MFH

MFH

SFH

 $4 \times SFH$

4. Results and Discussions

This section presents the results generated by applying the proposed control architecture to the case study simulation introduced before.

4.1. **VPP operation** – **Peak shaving.** Figure 3 shows the active power flow at the slack bus when the cooperation mechanism is implemented (3a) and not implemented (3b) during winter time, considering a standard day-night electricity tariff profile (Table 2). It is shown that the DMPC algorithm is successfully maintaining the aggregated load curve in between the predicted bounds with the exception of a few overshoots. These violations are correlated to strong prediction errors in the uncontrollable electricity consumption which highly influence the performance of MPC. Since a cost based performance index has been considered (Eq. 1), the different MPC regulators tend to maximize their power consumption during low electricity tariff periods (i.e. night time), hence creating virtual consumption peaks. The totally independent control MPC formulation performed without any coordination particularly reflects this undesired effect with peaks reaching 27 kWe at the slack bus. In order to face this issue, a global power flow constraint of ± 15 kWe has been added to the optimization problems to attenuate the load spikes (Figure 3b). Figure 3c finally shows the aggregated state of charge (SoC) of the thermal and electrical storage units monitored by each MPC. During low tariff periods, the controllers heavily charge the domestic hot water (DHW) tanks and batteries to satisfy local (i.e. comfort and operating costs) and global (i.e. load constraints) objectives. Moreover, since the feed-in tariff of electricity is lower than the night market price (Table 2), the MPC regulator tries to maximize self-consumption and the excess PV power generation is recovered by the electrical and thermal storage systems.

In order to analyze the DMPC performance with respect to seasonal variations, Figure 4 presents the active power profile when performing DMPC (4b) and when considering only local objectives (4a), during summer time. Regarding the large power generation resulting from the different RESs installed, the electrical storage capacity (Figure 4c) is not sufficient to satisfy

Building type	Heating		\mathbf{RES}	
building type	Unit	Type	Unit	Size
SFH	Heat Pump	Air-Water	PV panel	$50 \ [\mathrm{m}^2]$
MFH	Heat Pump	Air-Water	-	
$4 \times SFH$	Boiler	Natural Gas	PV panel	$100 \; [\mathrm{m}^2]$
SFH	Heat Pump	Air-Water	PV panel	$35 \; [\mathrm{m}^2]$
MFH	Cogeneration	Natural Gas	-	
	Thermal Storage		Electrical Storage	
	Unit	Size	Unit	Size

34.8 [kWh]

69.7 [kWh]

46.4 [kWh]

69.7 [kWh]

Battery Stack

Battery Stack

Battery Stack

3 [kWh]

12 [kWh]

2 [kWh]

Hot Water Tank

Hot Water Tank

Hot Water Tank

Hot Water Tank

Table 1. Parameters for the distributed energy system (DER).

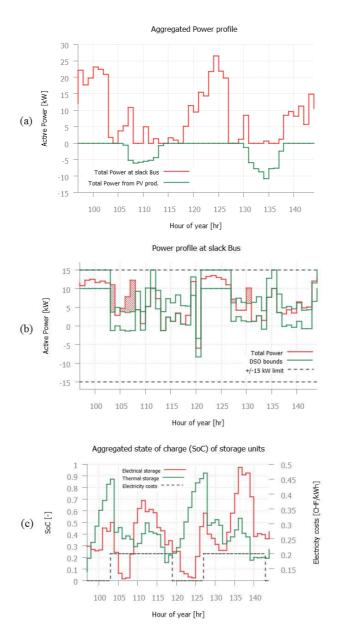


FIGURE 3. MPC problem formulation comparison for 3 typical winter days. Active power profile at the grid slack bus without (a) and with (b) MPC coordination, as well as the state of charge for aggregated storage unit (c).

the peak shaving constraint introduced previously. The power consumption/generation curve indeed exceeds the ± 15 kWe threshold since thermal storage through spacing heating and the hot water tank (that saturates over time) is not available during this period of the year, the excess of power must be reinjected into the distribution grid. To address this issue, long-term, seasonal storage may be necessary through a larger, centralized system located next to the slack bus.

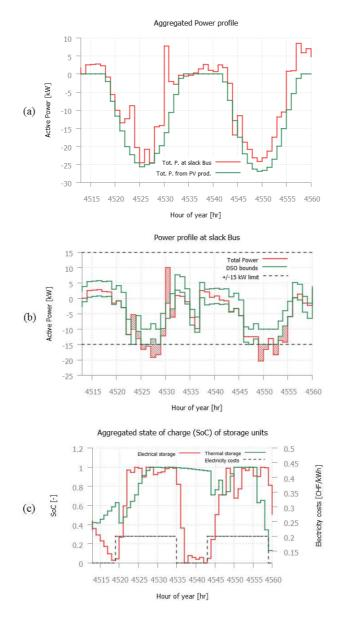


FIGURE 4. MPC problem formulation comparison for 3 typical summer days. Active power profile at the grid slack bus without (a) and with (b) MPC coordination, as well as the state of charge for aggregated storage unit (c).

4.2. **24h-ahead Tariff for Load Shifting.** As stated previously, regarding the specific performance index considered (Eq. 1), the different MPC controllers maximize power consumption during low tariff periods. Hence, in order to steer electricity imports towards specific periods of the day, the DSO might provide the ISO with specific day-ahead market prices prior the computation of the 24 hours load prediction. Since the MPC targets are entirely costs based, the local DSO may thus be able to shape the aggregated consumption profile regarding its current interest. Figure 5 shows the consumption strategy computed by the distributed control scheme,

Import price Export price Tariff $[CHF/kWh_e]$ $[CHF/kWh_e]$ 7 am - 10 pm 0.24Day-Night 0.1 else0.135 pm - 11 am 0.2124h-ahead 0.1else0.16Violation costs $[CHF/kW_e]$ Predicted profile Global power 0.5 0.25

Table 2. Variable electricity tariff profiles.

during spring time, while setting lower import costs during mid-day periods, when power generation from RESs is peaking (Table 2). Indeed, the maximum of the aggregated power flow curve is shifted towards the desired time frame, thus, providing the DSO with an additional ancillary service, that is load shifting.

Table 3 presents the performance values of both pricing schemes considered in this study (Figure 5). As expected, the mean power flow (at the slack bus) during low tariff periods is higher than the one during low price periods. As stated previously, the total bound violations are related to prediction errors, mainly for the outer conditions. Indeed, the overshoots occurring in the morning time are caused by the change in the minimum comfort temperature within the buildings and thus, are linked to the outside temperature. However, the peaks observed in Figure fig:ahead a are considerably limited since the controllers used the storage systems which have been fully charged during the preceding low tariff period (i.e night). A similar behavior can be noticed for the strong undershoot in Figure 5b; regarding previous low price period (i.e mid-day), the regulators could not provide sufficient storage capacity in order to recover the unpredicted, generated power excess.

Nevertheless, although no grid operation constraints have been included in the local performance, an a posteriori power flow analysis shows that the voltage and phase angle remain

TABLE 3. DMPC performance for day-night and 24h-ahead tariffs during spring time.

Tariff	Mean power flow $[kW_e]$		Total	
	Low tariff	High tariff	$[\mathrm{kWh}_e]$	
Day-night	10.76	1.78	202	
24h-ahead	7.88	2.77	181.3	
	Bound vio	olation $[kWh_e]$	${\bf Relative} \; [\text{-}]$	
	Bound vio	$\frac{\text{olation } [\text{kWh}_e]}{\text{Mean}}$	Relative [-] Total	
Day-night				

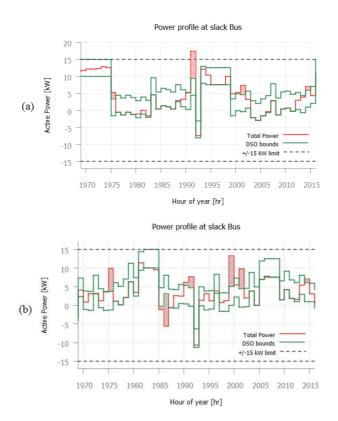


FIGURE 5. MPC problem formulation with a modified tariff profile (Table 2). Active power profile at the grid slack bus with the standard day-night (a) and the 24h—ahead (b) tariff.

within a standard quality limit of ± 5 p.u. (Table 4). In order to account for the fast dynamics of electrical DERs and hence, their optimal operation, a second control layer should indeed be considered during future development. As proposed in [14] for systems with different dynamics, a hierarchical approach can be added to the actual MPC problem formulation. The second control level evaluates the set points of electrical energy systems with a smaller sample time (5-15 minutes) in order to maintain the grid quality within the desired bounds (± 5 p.u.). However, to cope with dynamics at higher frequencies (e.g. solar irradiance variations), real-time control must still be implemented, which relies outside of the scope of this paper. Curious reader is referred to [19].

Table 4. Maximal voltage and angle deviation during DMPC operation.

2.2 4.6

5. Conclusions

This paper has presented flexible and modular control architecture to define the optimal operation plans of DERs connected to a microgrid. Based on an iterative, independent and fully connected MPC problem formulation, the presented approach enables VPP operation through a central ISO, while providing ancillary services to the local DSO. The case study simulation results showed the performance of the proposed control scheme; although a few overshoots have been noticed particularly due to strong prediction errors, the coordinating MPC regulators have successfully steered towards the desired operation plan. In addition, the latter simulation showed the flexibility of the DMPC to steer the aggregated power profile towards specific periods through day-ahead market tariffs defined by the DSO.

Future studies are planned to investigate the optimal design of the energy systems installed at each building with respect to the presented case study which has not been shown in this paper. Moreover, pricing strategies related to transgressions of the forecasted load curve might also be proposed. In fact, in case of constraint violation, the resulting penalty is preserved by the ISO, however the latter entity solely represents the aggregated interest of the different DERs and the DSO without providing any services or operating strategies.

References

- [1] P.P. Varaiya, F.F. Wu, and J.W. Bialek, Smart operation of smart grid: Risk-limiting dispatch. Proceedings of the IEEE (2011), vol. 99, pp. 40–57.
- [2] F. Kennel, D. Görges, and S. Liu, Energy Management for Smart Grids With Electric Vehicles Based on Hierarchical MPC, IEEE Transactions on industrial informatics (2013), vol. 9, pp. 1528–1537.
- [3] R.P. Menon, M. Paolone, and F. Maréchal, Model predictive control strategies for low-voltage microgrids. Presented in conference On Process Integration, Modelling And Optimisation For Energy Saving And Pollution Reduction, Aidic Servizi Srl (2014), vol. 39, no. EPFL-CONF-205229, pp. 1123–1128.
- [4] M. Bosetti, Operation of distributed networks with distributed generation, Ph.D. Dissertation, Dept. Electrical Eng., University of Bologna, Bologna, 2009.
- [5] F. Katiraei, R. Iravani, N. Hatziargyriou, and A. Dimeas, Microgrid management, IEEE power & energy magazine (2008), vol. 6, pp. 54–65.
- [6] N. Hatziargyriou, A. Dimeas, and A. Tsikalakis, Centralized and Decentralized Control of Microgrids, Int. Journal of Distributed Energy Resources (2005), vol. 1, pp. 197–212.
- [7] A. Borghetti, M. Bosetti, S. Grillo, S. Massucco, C. A. Nucci, M. Paolone, and F. Silvestro, Short-Term Scheduling and Control of Active Distribution Systems With High Penetration of Renewable Resources, IEEE Systems Journal (2010), vol. 4, pp. 313–322.
- [8] P.O. Kriett and M. Salani, Optimal control of a residential microgrid, Enegry (2012), vol. 42, pp. 321-330.
- [9] A. Collazos, F. Maréchal, and C. Gähler, Predictive Optimal Management Method for the Control of Polygeneration Systems, Computers and Chemical Engineering (2009), vol. 33, pp. 1584–1592.
- [10] H. Dagdougui, R. Minciardi, A. Ouammi, M. Robba, and R. Sacile, Modeling and optimization of a hybrid system for the energy supply of a green building, Energy Conversion Management (2012), vol. 64, pp. 351– 363.
- [11] G.P. Henze, D.E. Kalz, S. Liu, C. Felsmann, Experimental analysis of model-based predictive optimal control for active and passive building thermal storage inventory. HVAC&R Research (2005), vol. 11, 189–213.
- [12] G.T. Costanzo, J. Parvizi, and H. Madsen, A Coordination Scheme for Distributed Model Predictive Control: Integration of Flexible DERs, In Proceedings of IEEE ISGT conference (2013), pp. 1–5.
- [13] A. Richards and J. P. How, Robust distributed model predictive control, Int. Journal of Control (2007), vol. 80, pp. 1517–1531.
- [14] R. Scattolini, Architectures for distributed and hierarchical Model Predictive Control A review, Journal of Process Control (2009), vol. 19, pp. 723–731.
- [15] S. Papathanassiou, N. Hatziargyriou, and K. Strunz, A Benchmark Low Voltage Microgird Network, Presented at the CIGRE Symposium, 2005.

- [16] D. Jia and B. Krogh, Distributed Model Predictive Control, In Proceedings of American Control Conference (2001), pp. 2767–2772.
- [17] A. Ashouri, Simultaneous Design and Control of Energy Systems, Ph.D. Dissertation no. 21908, ETH Zurich, 2014.
- [18] S. Fazlollahi, G. Becker, A. Ashouri, F. Maréchal: Multi-objective, multi-period optimization of district energy systems: IV-A case study. Energy (2015), vol. 84, pp. 365–381.
- [19] A. Bernstein, L. Reyes-Chamorro, J.Y. Le Boudec, and M. Paolone, A Composable Method for Real-Time Control of Active Distribution Networks with Explicit Power Setpoints. Part I: Method, Electric Power Systems Research (2015), vol. 125, pp. 265–280.